JOURNAL OF MATERIALS SCIENCE 32 (1997) 1195–1199

The influence of the structure on the electrical and magnetic properties of $Bi_2Sr_2CaCu_2O_{8+\delta}$ single crystals

G. ALDICA, A. CRISAN, M. VELTER-STEFANESCU, S. MANDACHE
Institute of Physics and Technology of Materials, P.O. Box MG-7, Bucharest, Romania
M. C. BUNESCU
METAV SA, P.O. Box 18/3, Bucharest, Romania

The correlation between the structure, chemical composition, electrical and magnetic properties of $Bi_2Sr_2CaCu_2O_{8+\delta}$ single crystals is presented. As revealed by SEM measurements, the small samples (approximately 1 mm × 1 mm × 0.2 mm) are stacks of thin plates (1–2 μm). Microcompositional measurements (energy dispersive spectroscopy) show the $Bi_2Sr_2CaCu_2O_{8+\delta}$ (2212)-phase and a small quantity of residual phases enriched in bismuth and strontium and calcium-deficient. Magnetically modulated microwave absorption measurements (MAMMA) lead to a value for the anisotropy of the upper critical field of about 7, which is more than twice the reported value for $YBa_2Cu_3O_{7-\delta}$ single crystals (also determined from MAMMA responses). The plot of the resistance versus temperature suggests that only the first 10–20 plates from the surface of the sample have a contribution to the sample conductivity. The imaginary part, χ'', of the magnetic susceptibility of our samples shows three peaks.

1. Introduction

Since the discovery of superconductivity in the Bi–Sr–Ca–Cu–O system, various relationships between the structure of the single crystals (obtained with different growth methods), and the electrical and magnetic properties, have been proposed [1–5]. As is well known, the above-mentioned system has three superconducting phases: $Bi_2Sr_2CuO_{6+x}$ (2201), $Bi_2Sr_2CaCu_2O_{8+y}$ (2212) and $Bi_2Sr_2Ca_2Cu_3O_{10+z}$ (2223) with critical temperatures, T_c, of about 10, 80 and 110 K, respectively. Unfortunately, single crystals from the 2223 phase (with the highest T_c) have not yet been produced and, moreover, it is still difficult to produce 2212 single crystals with reasonable thickness ($\geqslant 1$ mm).

In this work, attempts were made to correlate the structure and composition of the 2212 single crystals, determined by scanning electron microscopy (SEM) and by energy dispersive spectroscopy (EDS), respectively, with a.c. susceptibility measurements, magnetically modulated microwave absorption measurements (MAMMA) spectra and theoretical modelling of the resistivity versus temperature $R(T)$ curves.

2. Experimental procedure

The $Bi_2Sr_2CaCu_2O_{8+\delta}$ single crystals were produced by the standard self-flux method [6] at the Department of Mechanical Engineering, II University of Rome.

Small samples with surfaces of a few square millimetres and thickness 40–200 μm were cleaved from the as-grown single-crystals conglomerate, which had approximately 0.5 cm^3 volume. The microstructure and microcomposition of the crystals were analysed using a Philips SEM-515 scanning electron microscope equipped with X-ray spectrometers (EDS and WDS).

The $R(T)$ curves were measured between 77 and 300 K, with different transport currents, using the standard four-probe method. The electric contacts were produced with silver paste, then heated at 500 °C for 30 min in air. The transport current densities through the samples were between 0.032 and 0.06 A cm^{-2}.

The microwave investigations were carried out in the X-band (9 GHz) at an incident microwave power of 5 mW by the MAMMA method [7, 8]. The MAMMA responses were registered in 5 mT d.c. magnetic field and in 0.1 mT a.c. magnetic field (100 kHz), slowly increasing the sample temperature (≈ 1 K min^{-1}) from 77 K up to 90 K. The selected single crystal ($0.8 \times 0.8 \times 0.2$ mm^3) was placed in the centre of a TE_{011} resonant cavity (where the microwave magnetic component is maximum) with the flat surface (*ab* plane) parallel to the axis of polarization of the microwave magnetic field (the vertical axis). The d.c. and a.c. magnetic fields were in the horizontal plane. As the microwave electric field vanishes at the sample, the primary source of microwave loss is due to

0022–2461

the eddy currents induced by the microwave magnetic field. These currents circulate in a plane perpendicular to the *ab* (conduction) plane of the sample.

The temperature dependence of the magnetic susceptibility was measured inductively, with a Hartshorn-type bridge, at an a.c. magnetic field, $H_{a.c.}$ of 15 kHz, with amplitudes between 0.0125 and 1.25 Oe. The samples were placed with the *ab* plane perpendicular to the magnetic field. The $\chi'(T)$ and $\chi''(T)$ curves were registered in field-cooling conditions, with a cooling rate in the superconducting transition range of about 2 K min^{-1}.

3. Results and discussion

3.1. Microstructural analysis

Fig. 1 represents a split image of the same area of the "as-cleaved" surface of the sample. The left side is a backscattered electron image (BEI) showing differences of contrast produced by different chemical compositions. The right side is a secondary electron image (SEI) showing a relatively flat surface with a few steps produced by the cleavage. Thus, even if the topography of the surface does not reveal any inhomogeneity, they exist in the areas with a light-grey contrast. These represent zones with a higher average atomic number than the rest of the material showing a grey contrast. The dark lines in the BEI image represent the steps observed in the SEI image.

The energy-dispersive X-ray microanalysis of different contrast areas in Fig. 1 shows that the light-grey zones have a smaller content of calcium and copper, and an increased content of bismuth and strontium than the rest of the material. The results are presented in Table I.

The same inhomogeneity could be observed when X-ray maps of BiM_α, SrL_α, CaK_α and CuK_α were analysed (Fig. 2a–d). One can observe (Fig. 2c and d) the smaller densities of points in the light-grey

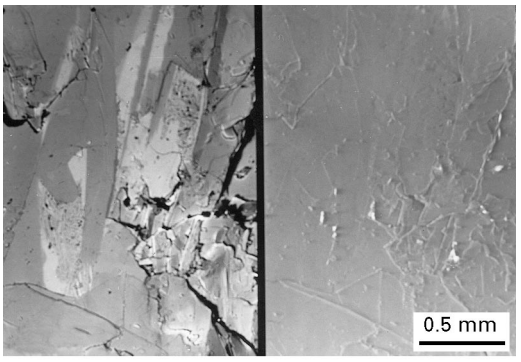

Figure 1 (a) BEI and (b) SEI of the surface of a 2212 crystal.

TABLE I EDS results obtained at different points of a 2212 crystal.

Point of analysis	Chemical composition (bal. O_2) (at %)				Cation ratio
	Bi	Sr	Ca	Cu	
Light-grey contrast	20.43	12.75	2.89	8.82	2.32:1.44:0.33:1
Light-grey contrast	18.86	20.59	0.76	5.08	3.71:4.05:0.15:1
Grey contrast	14.45	11.05	7.19	13.70	2.10:1.60:1.04:2
Grey contrast	14.25	11.47	7.23	13.49	2.10:1.70:1.08:2

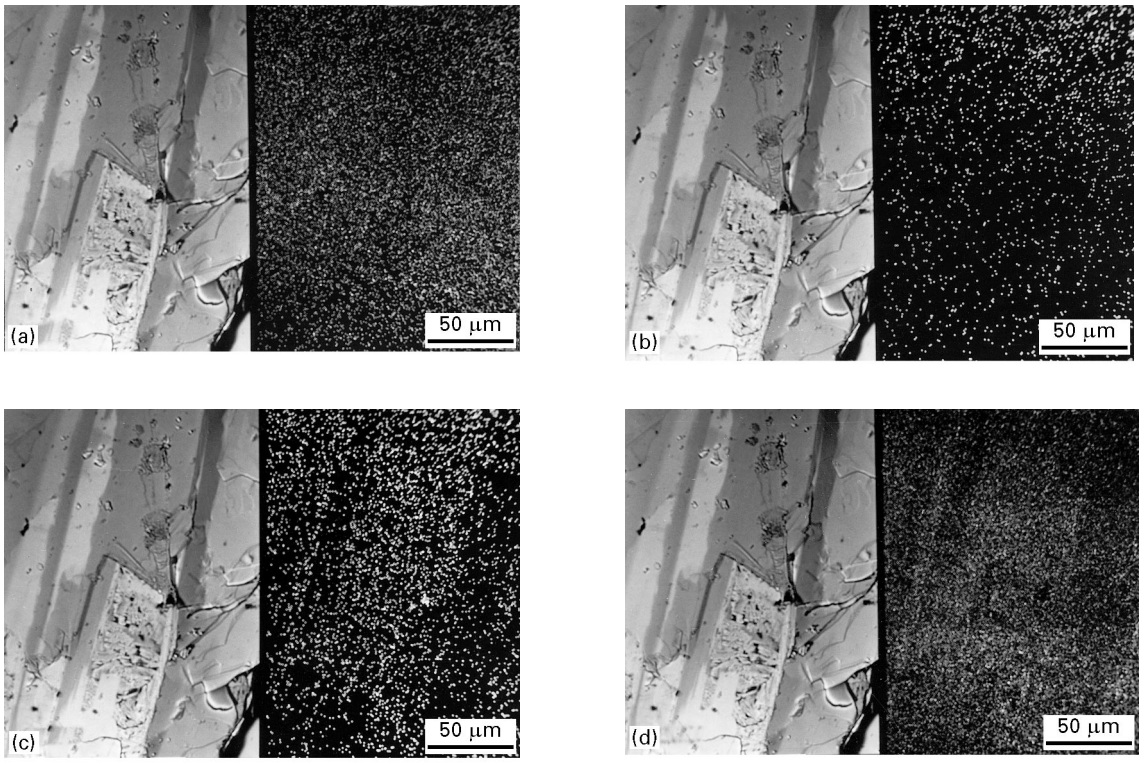

Figure 2 X-ray map of (a) BiM_α; (b) SrL_α; (c) CaK_α; (d) CuK_α radiation on the respective area.

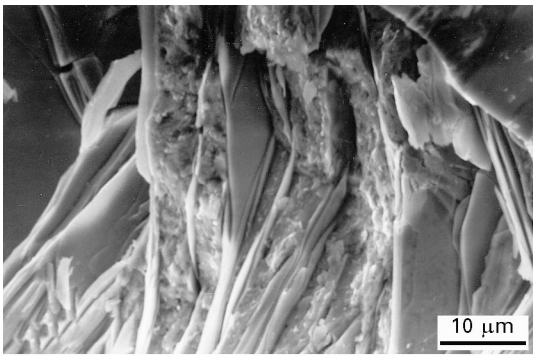

Figure 3 SEM image of the sample showing cleavage steps.

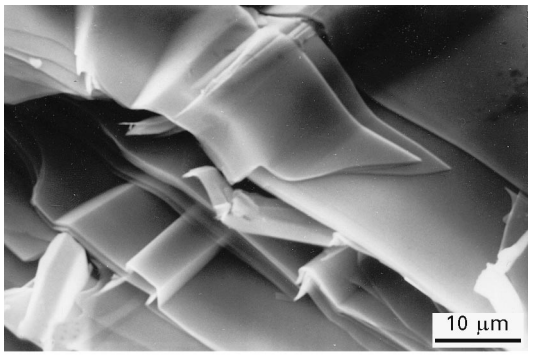

Figure 4 The lateral SEM image of 2212 crystal with the step structure.

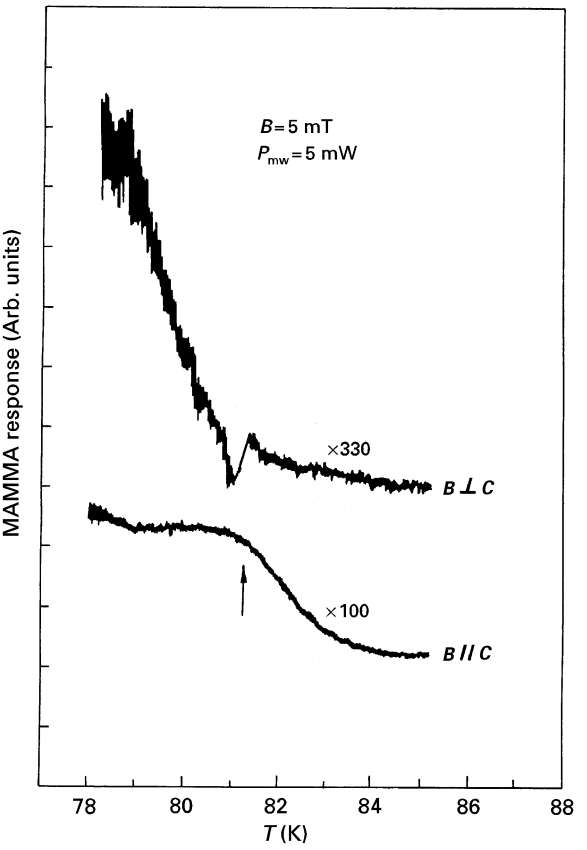

Figure 5 The MAMMA response in d.c. magnetic field parallel and perpendicular to the *c* axis.

contrast zones (the surface of the sample is flat enough to give reliable X-ray distribution).

A structure as in Fig. 3 was observed when the transverse fracture surface of a sample was analysed. Thin plates, 1–2 μm thick, alternate with layers of a residual phase. The EDS composition of this layer was 19.86 at % Bi, 12.13 at % Sr, 3.49 at % Ca and 9.55 at % Cu (2.08 : 1.27 : 0.36 : 1). It is obvious that this residual phase and the inhomogeneity observed in the planar view have the same cation ratio.

The clean edge of the sample shows a thin plate structure of 2212 phase, 1–2 μm thick, and no layer of residual phase (Fig. 4). The bridges can be allocated to the twin patterns on the (0 0 1) surface, also reported by other authors [3], who explained this morphology by the absorption of solid impurity particles, the structure growing subsequently free.

3.2. Microwave absorbtion measurements

In Fig. 5, the MAMMA responses in d.c. magnetic field (a) parallel and, (b) perpendicular to the *c* axis are shown. Both MAMMA peaks indicate an average critical temperature of about 81.2 K. The ratio of the MAMMA peak intensities for the *c* axis parallel and perpendicular to the magnetic field gives the ratio of the upper critical fields, H_{c2}, parallel (p) and normal (n) to the CuO_2 bilayers [9]

$$I_{\parallel}/I_{\perp} = H_{c2}(\mathrm{p})/H_{c2}(\mathrm{n}) \qquad (1)$$

The experimental value of this ratio is about 7, more than double that in the case of high-quality $YBa_2Cu_3O_{7-\delta}$ single crystals, for which the ratio determined by the same method was found to be 3 [9, 10].

Another experimental fact shown in Fig. 5 is the rising line below T_c, which indicates the presence of a great number of "intergrain" Josephson junctions. This means that the crystal contains many defect (non-superconducting) planes. Thus, the crystal can be considered as a stack, along the *c* axis, of well-oriented superconducting layers (in fact, very thin single crystals), which is in agreement with the microstructural observations.

3.3. Electrical measurements

In Fig. 6, the temperature dependence of the excess conductivity, $\Delta\sigma$, on a double-logarithmic scale, is presented. In the equation of the reduced temperature

$$t = (T - T_{cm})/T_{cm}, \qquad (2)$$

T_{cm} was determined at the intersection between the temperature axis and the extrapolation of the most pronounced drop in resistivity ($T_{cm} = 84.1$ K). The critical temperature is 87.7 K, while the transition width is about 13 K.

The fitting of the "S"-shaped curve in Fig. 6, which was done in the frame work of the thermodynamic fluctuations theory, reveals the existence of two-dimensional and three-dimensional superconductivity only in some selected temperature domains. For $\log_{10}(t) < -2$ the results are extremely dependent on the error in measuring (or selecting) T_c [11], so we

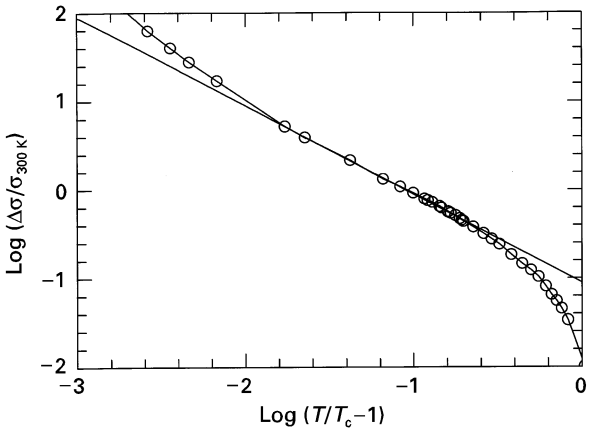

Figure 6 The reduced temperature dependence of the excess conductivity. (——) An attempted fit with the Aslamasov–Larkin two-dimensional model.

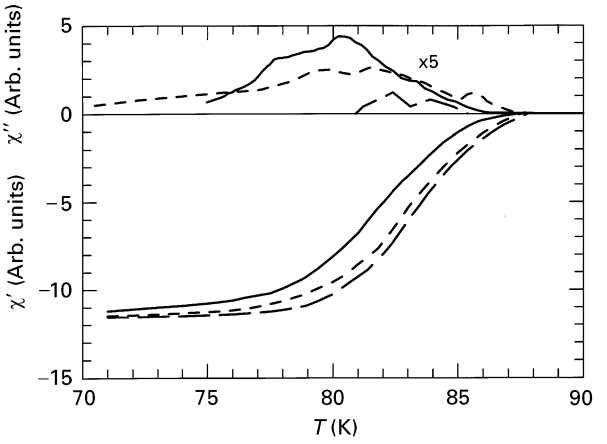

Figure 8 Temperature dependence of the a.c. susceptibility, for applied magnetic fields of 0.0125, 0.125 and 1.25 Oe.

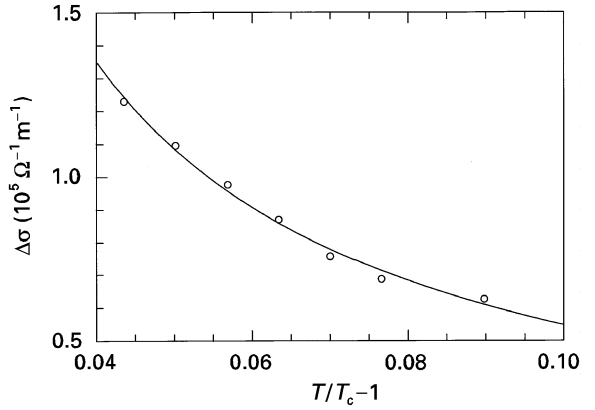

Figure 7 Temperature dependence of the excess conductivity fitted with the Lawrence-Doniach model (——).

performed the fitting only for temperatures not very close to T_c ($\log t > -2$). The full line in Fig. 6 represents, on a double-logarithmic scale, for $-1.8 < \log t < -0.8$, a fit with the Aslamasov–Larkin two-dimensional model, $\Delta\sigma \propto t^{-1}$.

We studied the excess conductivity also in the framework of the Lawrence–Doniach model [12] for layered superconductors (stacks of quasi-two-dimensional superconducting planes, with Josephson-type coupling in the direction normal to the planes). The existence of the two-dimensional superconductivity can be checked, in this model, by fitting the experimental data with the equation

$$\Delta\sigma_{LD}(T) = (e^2/16\hbar st)[1 + (2\xi_c(0)/s)^2/t]^{-1/2} \quad (3)$$

where s is the spacing between the superconducting (ab) planes and $\xi_c(0)$ is the coherence length along the c axis.

An attempted fit with equation 3 is presented in Fig. 7, for $0.04 < t < 0.1$. From the two fitting parameters we obtained the interlayer spacing $s \approx 2.76$ nm and the coherence length $\xi_c(0) \approx 0.06$ nm, while the value reported in the literature [2, 13] is $s \approx 1.5$ nm. With $\xi_{ab}(0)$ reported in [2, 13] and the anisotropy factor determined elsewere [14], the generally accepted value of the coherence length along the c axis is $\xi_c(0) \approx 0.015$ nm [15]. We assume that this difference is due to the fact that, in the case of our sample and with the four contacts on the same side of the sample, only the first 10–20 single-crystal plates have contributions to the electrical conductivity. Indeed, if we take into the calculation of $\Delta\sigma$ a sample thickness of 20 μm instead of the real value of about 40 μm, the resulting s is very close to the real one. The error in determining $\xi_c(0)$ is, however, large, because the second term in Equation 3 has a minor contribution, perhaps of the same order of magnitude as the experimental errors.

3.4. A.c. susceptibility

The real and imaginary terms of the diamagnetic response were recorded for temperatures between 60 and 300 K. Some results are presented in Fig. 8. The onset critical temperature for the diamagnetic response is 88 K, while the saturation of the Meissner effect appears at about 75 K. The diamagnetic transition width of about 5 K is much smaller than the width of the resistive transition (13 K). One can see that the influence of the amplitude of the magnetic field on the shape of the $\chi'(T)$ dependence is more pronounced at higher amplitudes.

The imaginary part of the a.c. susceptibility was quite difficult to measure, especially in weak magnetic fields. Anyway, the $\chi''(T)$ dependence shows three broad peaks (very clear for $H_{a.c.} = 0.125$ Oe). The signal (dissipation) increases with increasing field, which is normal. For $H_{a.c.} = 0.0125$ Oe, the high-temperature peak is not observed from the background signal. This shape of the $\chi''(T)$ dependence can be correlated with the sample's structure. The high-temperature peak is related to the persistent currents circulating in the superconducting ab planes. The main loss is connected with the central peak and we believe that this is due to the currents circulating in a single-crystal plate, while the third peak can be correlated with the currents circulating between neighbouring superconducting plates (of 1–2 μm thickness). The different field dependence of the heights of the three peaks shows a different contribution of these types of persistent current with changing

temperature. As the field increases, the central peak becomes more important, while the other two become more like shoulders of the central one. At higher fields, the $\chi''(T)$ dependence moves to lower temperatures. All these aspects are consistent with the complexity of the superconducting plate structure of the sample, the different types of junction playing a very important role in the a.c. susceptibility.

4. Conclusion

The correlation between the structure and chemical composition of $Bi_2Sr_2CaCu_2O_{8+\delta}$ single crystals has been studied. The samples consist of stacks of thin single-crystal plates (1–2 μm thick). The plate boundaries are either "clean" or consist of residual phases bismuth- and strontium-rich and calcium-deficient, as revealed by SEM and EDS measurements.

The critical temperatures determined by resistivity measurements, a.c. susceptibility and magnetically modulated microwave absorption are 87.7, 88 K (onset) and, respectively, 81.2 K. The ratio $H_{c2}(H_a \perp c)/H_{c2}(H_a \| c) = 7$ is twice the reported value for $YBa_2Cu_3O_{7-\delta}$ single crystals (also determined from MAMMA responses).

For $1.04T_c < T < 1.1T_c$ the excess conductivity is described very well by the Aslamasov–Larkin and Lawrence–Doniach two-dimensional models. The interlayer spacing and the coherence length were obtained from the fitting parameters, and their deviation from the generally accepted values was explained by the small number of single-crystal plates that contribute to the conductivity.

The a.c. susceptibility measurements revealed different types of junctions, with different responses and critical temperatures.

References

1. S. MARTIN, A. T. FIORY, R. M. FLEMING, G. P. ESPINOZA and A. S. COOPER, *Appl. Phys. Lett.* **54** (1989) 72.
2. *Idem*, *Phys. Rev. Lett.* **62** (1989) 677.
3. Y. WANG, P. BENNEMA, L. W. M. SCHREURS, J. WRUCK and P. VAN DER LINDEN, *Appl. Phys. A* **52** (1991) 548.
4. G. BRICERO, M. F. CROMMIE and A. ZETIL, *Phys. C* **204** (1993) 389.
5. A. J. S. CHOWDHURRY, B. M. R. WANKLIN, F. R. WONDRE, J. W. HODBY, A. V. VOLKOZUB and P. A. J. DE GROOT, *ibid.* **225** (1994) 388.
6. G. BALESTRINO and P. PAROLI, private communication.
7. K. MOORJANI, J. BOHANDY, F. J. ADRIAN, B. F. KIM, R. D. SHULL, C. K. CHIANG, L. J. SWARTZENDRUBER and L. H. BENNETT, *Phys. Rev. B* **36** (1987) 4036.
8. B. F. KIM, J. BOHANDY, K. MOORJANI and F. J. ADRIAN, *J. Appl. Phys.* **63** (1988) 2029.
9. D. SHALTIEL, H. BILL, A. GRAYEVSKY, A. JUNOD, D. LOVY, S. SADOWSKI and E. WALKER, *Supercond. Sci. Technol.* **4** (1991) S85.
10. W. BAUHOFER, W. BIBERACHER, B. GEGENHEIMER, W. JOSS, R. K. KREMER, H. J. MATTAUSCH and A. SIMON, *Phys. Rev. Lett.* **63** (1989) 2520.
11. R. HOPPENGÄRTNER, B. HENSEL and G. SAEMANN-ISCHENKO, *Phys. Rev. B* **44** (1991) 741.
12. L. G. ASLAMASOV and A. I. LARKIN, *Phys. Lett.* **26A** (1968) 238.
13. W. E. LAWRENCE, S. DONIACH, in "Proceedings of the 12th International Conference on Low Temperature Physics", edited by E. Kanda (Keigaken, Tokyo, 1971) 361.
14. S. A. SUNSHINE, T. SIEGRIST, L. F. SCHNEEMEYER, D. W. MURPHY, R. L. CAVA, B. BATLOGG, R. B. VAN DOVER, R. M. FLEMING, S. H. GLARUM, S. NAKAHARA, R. FARROW, J. J. KRAJEWSKI, S. M. ZAHURAK, J. V. WASZSCAK, J. H. MARSHALL, P. MARSH, L. W. RUPP Jr and W. F. PECK, *Phys. Rev. B* **38** (1988) 893.
15. L. MIU, P. WAGNER, A. HADISH, F. HILLMER and H. ADRIAN, *Phys. C* **234** (1994) 249.

Received 16 February
and accepted 31 July 1996